1

The Chemical Principles of RNA Catalysis

Timothy J. Wilson and David M. J. Lilley

The University of Dundee, Cancer Research UK Nucleic Acid Structure Research Group, MSI/WTB Complex, Dow Street, Dundee DD1 5EH, UK

1.1 RNA Catalysis

Ribozymes are enzymes that are made of RNA rather than protein. Their function is to accelerate the rates of chemical reactions. This chapter discusses the chemical principles of catalysis as applied to biological macromolecules. Except for the peptidyl transferase reaction of the ribosome, the known natural ribozymes all carry out phosphoryl transfer reactions, either transesterification (including nucleotidyl transfer) or hydrolysis. We shall therefore focus on these reactions principally. However, RNA can bind small molecules with great selectivity, and indeed the riboswitches exploit this ability in many ways to control gene expression. One, the glmS (glucosamine-6-phosphate riboswitch) ribozyme, uses a bound molecule as a coenzyme, and it is not impossible that other ribozymes that use coenzymes in a wider range of chemistry remain to be discovered. Ribozymes that have been selected in the laboratory demonstrate that a wider range of chemistry can be supported by RNA catalysis [1–3].

One of the most powerful tools that we can use to study the ribozyme mechanism is X-ray crystallography. Having a knowledge of the three-dimensional structure is invaluable. Yet this is not enough and may even be misleading. This may happen for several possible reasons. First, the RNA sequence may have been reduced too far, removing key elements required for proper structure and function. This occurred with the hammerhead ribozyme [4], where the removal of critical elements that formed a tertiary interaction led to a remodeling of the active center [5]. The active species is rarely studied. The structure of the ribozyme has often been modified to prevent activity, and the possible consequences of the modification need to be considered. Second, crystal contacts may induce structural changes, as found in the twister ribozyme where the nucleotide 5′ to the scissile phosphate was pulled out of the active site by interaction with guanine in a symmetry-related ribozyme molecule leading to loss of an in-line geometry [6]. Lastly, of course, a crystal structure can never capture the transition state because, by definition, it is fleeting. The best we

Ribozymes, First Edition. Edited by Sabine Müller, Benoît Masquida, and Wade Winkler.

can do is to find a related high-energy intermediate if it exists or try to model it with a transition state analog as was done for the hairpin [7] and hammerhead [8] ribozymes. But we always need to apply chemical insight when looking at crystal structures of ribozymes, and frequently we must extrapolate what we find to deduce the events occurring in the transition state. Ultimately only kinetic measurements probe transition state properties. It is thus the combination of structural analysis, kinetic measurements, and atomic mutagenesis that allow us to approach an understanding of the catalytic chemical mechanism.

1.2 Rates of Chemical Reactions and Transition State Theory

The possible trajectory of a chemical reaction is described by a potential energy surface plotting the free energy at each point on the reaction landscape. The reaction will take the path of lowest free energy between the starting material and product, and the highest point along that path is the transition state, generally described as a saddle point on the reaction trajectory. In transition state theory [9–11], we calculate the rate of reaction as the concentration of the activated complex (i.e. the species at the point of highest free energy, or transition state) multiplied by the rate of passage out of that state that will be related to bond vibrational frequencies. An equilibrium between the ground state and transition state is postulated, leading to an expression for the rate (k) as

$$k = \kappa \cdot \left({}^{k_B T}/_{h}\right) \exp\left({}^{-\Delta G^{\ddagger}}/_{RT}\right) \tag{1.1}$$

where k_B is Boltzmann's constant, h is Planck's constant, R is the gas constant, and T is the absolute temperature. κ is a factor that measures the probability of the transition state proceeding to form the product. The key parameter here is $\Delta G^{\ddagger}$, which is the free energy of activation that must be supplied to promote the substrate to the transition state. The population of the activated complex thus governs the rate of reaction that will be determined by the energy barrier according to statistical mechanics. Parenthetically, we note that it is mechanistically valuable to be able to relate chemical rates to equilibrium properties, and that linear free energy relationships are very important in the analysis of catalysis.

Transition state theory shows that chemical catalysis is a question of reducing the energetic barrier to the formation of the activated complex, i.e. stabilizing the transition state to lower its free energy. This can occur in a variety of ways, including electrostatic interactions, stabilization by hydrogen bonding, and formation of covalent complexes. We shall discuss this further for the phosphoryl transfer reactions that occur in the ribozymes.

The activation free energy $\Delta G^{\ddagger}$ can, of course, be parsed into enthalpy and entropies of activation. The latter can be particularly important in bimolecular reactions, which involve the loss of translational and rotational entropy in the formation of the activated complex. Chemical catalysis occurs in two forms: homogeneous catalysis, where reactants and catalyst are in the same phase, and heterogeneous catalysis, where typically the reaction occurs on some surface. In

a sense, macromolecular catalysis is somewhat intermediate. When two reactants bind to a macromolecular catalyst, the loss of translational and rotational freedom is partially "paid for" in advance, and the effective concentration of the reactants is increased. Thus in peptidyl transferase reactions, the peptidyl- and aminoacyl-transfer RNAs (tRNAs) are bound to the ribosome and oriented ready to condense to form a new peptide bond. In the group, I intron ribozyme first stage reaction exogenous guanidine reacts when it is bound to the ribozyme. Activation entropy can also appear in more subtle ways, as the reorganization of solvent during the reaction, for example.

1.3 Phosphoryl Transfer Reactions in the Ribozymes

All the known natural ribozymes apart from ribosomal peptidyl transferase catalyze phosphoryl transfer, so we shall focus here on phosphoryl transfer reactions [12]. Figure 1.1 shows the reactions catalyzed by the nucleolytic ribozymes, and the group II and I self-splicing intron ribozymes. These are all transesterification reactions that involve the nucleophilic attack of a ribose hydroxyl group on the phosphodiester linkage of RNA. For the nucleolytic and group II ribozymes, the nucleophile is a 2′-hydroxyl, on the adjacent or a remote ribose, respectively. For the first stage of the group I ribozymes, the nucleophile is the 3′-hydroxyl of a guanosine molecule. In the case of RNaseP, the nucleophile is water, and the group II ribozyme can also undergo a hydrolytic reaction.

The phosphorus atom in a phosphodiester is tetrahedral, with four sp^3 orbitals bonded to two bridging and two non-bridging oxygen atoms. The $pK_a = 1$, so there is a negative charge; the bonds to the non-bridging O atoms have partial double bond character by pπ–dπ interaction, and the charge is delocalized. Nucleophilic attack of the oxygen of ROH or HOH requires the participation of the P d orbital, forming a phosphorane intermediate with sp^3d character that is close to the transition state (Figure 1.2a). The phosphorane is trigonal bipyramidal, with three equatorial O atoms and the nucleophilic and leaving group O atoms in the apical positions [14] (Figure 1.2b). Therefore to generate the phosphorane, the nucleophile must attack in-line with the P and the leaving group O.

The cleavage reaction for the nucleolytic ribozymes is shown in Figure 1.3. The products of the reaction are a cyclic 2′,3′-phosphate, and a 5′-hydroxyl. For the hammerhead and hairpin ribozymes, it has been demonstrated that the reaction proceeds with inversion of chirality at the phosphorus atom [15, 16]. This is consistent with the S_N2 mechanism shown, proceeding via the phosphorane. Kinetic isotope effects measured for the formation of cyclic 2′,3′-phosphate from uridine 3′-*m*′-nitrobenzyl phosphate [17] were indicative of a phosphorane-type transition state. Using a series of oligonucleotides containing a nucleoside analog with 2′-C-β-branched substituents with fluoro substitution having a range of pK_a values, Piccirilli and coworkers [18] measured the Brønsted parameter β_{nuc}. This gives a measure of the change in charge on the nucleophile approaching the transition state. Ye et al. obtained $\beta_{nuc} = 0.75 \pm 0.15$. The corresponding Brønsted

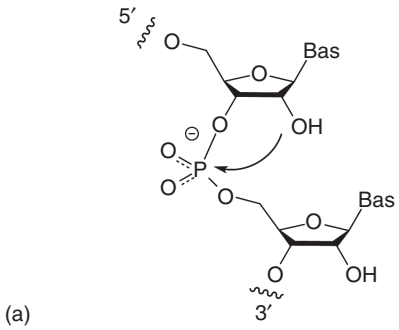

(a)

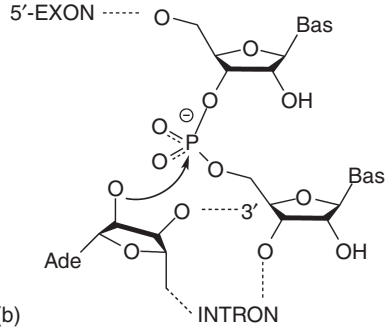

(b)

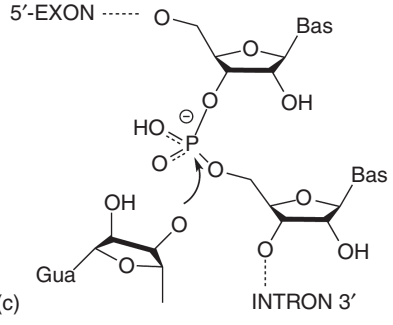

(c)

Figure 1.1 Three ribozyme-catalyzed transesterification reactions. In the nucleolytic ribozymes (a), the O2′ attacks the adjacent 3′-P with departure of the O5′. In the group II intron ribozyme (b), there is a similar reaction except that the O2′ nucleophile is remote within the intron. The nucleophile in the first reaction of the group I intron ribozyme (c) is the O3′ of an exogenous guanosine molecule.

parameter for the leaving group β_{lg} was measured by Lönnberg and coworkers [19] using a series of model uridine 3′-phosphate monoalkyl esters. They obtained $\beta_{lg} = -1.28 \pm 0.02$. These values are consistent with a concerted mechanism for the cleavage reaction, with significant development of charge on the oxygen atoms of the nucleophile and leaving groups.

1.4 Catalysis of Phosphoryl Transfer

We shall now consider how the cleavage reaction for the nucleolytic ribozymes could be catalyzed. These ribozymes achieve about a million-fold enhancement in rate

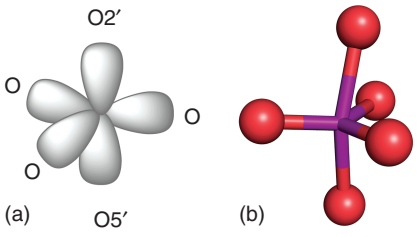

Figure 1.2 The geometry of a phosphorane. (a) A representation of phosphorus orbital hybridization in a phosphorane. The phosphorus atom is sp^3d hybridized and has trigonal bipyramidal geometry. (b) The structure of a vanadate transition state analog taken from the crystal structure of the hairpin ribozyme [13]. The vanadate mimics the conformation of the penta-coordinate phosphorane that is close to the transition state for the ribozyme transesterification reaction. The nucleophile and leaving group are in the apical positions, and three oxygen atoms lie in the central plane.

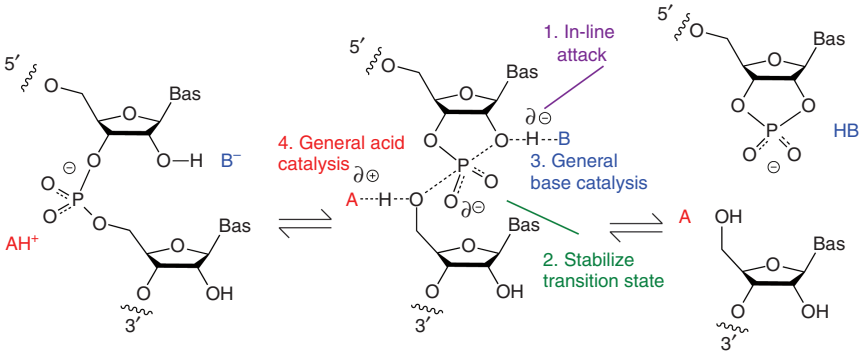

Figure 1.3 The chemical mechanism of the nucleolytic ribozymes and possible catalytic strategies. Cleavage proceeds left to right, and ligation right to left. The transition state is approximated by the central structure, with a pentavalent, trigonal-bipyramidal phosphorane structure. Four potential catalytic strategies are indicated. (1) is the in-line trajectory of attack, (2) stabilization of the transition state structurally or electrostatically, (3) deprotonation of the nucleophile, and (4) protonation of the oxyanion leaving group. By the principle of microscopic reversibility, this reaction scheme is symmetrical. For example, B^- acts as a general base to deprotonate the O2′ nucleophile in the cleavage reaction, and thus, BH acts as a general acid to protonate the O2′ leaving group in the ligation reaction, where O5′ is now the nucleophile.

over the reaction in a flexible dinucleotide, and a number of catalytic strategies may contribute to this; several authors have listed the potential contributions [20–22]. While this is a useful guide to our chemical thinking, in the end, everything comes down to stabilization of the transition state, i.e. lowering the activation barrier $\Delta G^{\ddagger}$ in Eq. (1.1). All the contributions are interconnected, and catalysis is multifactorial. With that caveat, we can consider four major contributions to catalysis of the phosphoryl transfer reaction (Figure 1.3).

1. *Alignment of nucleophilic attack*. As noted above, the nucleophile O, P, and leaving group O are aligned in the phosphorane, and the nucleophile must attack with

a trajectory that is co-linear with the P and the leaving O. A flexible dinucleotide will randomly sample the in-line geometry, but ribozymes are larger and structured. The required orbital overlap is not a sharp function of orientation, so some deviation from a perfect line of attack will be tolerated. Pre-alignment by the structure of a ribozyme may contribute a part of the total rate enhancement, but this is likely to be significantly less than 10^2. Of course, the RNA structure must not get trapped in a conformation that is markedly out of alignment – indeed, this is the basis of in-line probing of RNA structure [20].

2. *Structural and/or electrostatic stabilization of the transition state*. Two aspects of the phosphorane distinguish it from the substrates and products, i.e. a change in the conformation and a redistribution of electric charge. In principle, if the RNA is, to some degree, complementary to the structure of the transition state, it may stabilize it by the formation of interactions not found in the ground state. We have noted an example in the twister ribozyme, where a stereospecific hydrogen bonding interaction between a guanine N2 and a non-bridging O atom of the scissile P leads to a 100-fold difference in cleavage rate [22]. The phosphorane is formally dianionic, and the juxtaposition of positive charge could stabilize the charge redistribution. In principle, this might be that of a metal ion or nucleobase, or due to proton transfer as discussed in the following section 1.5.
3. *Deprotonation of the nucleophile*. The value of the Brønsted parameter β_{nuc} [18] indicates that there is a significant accumulation of positive charge on the O2′ nucleophile, and this could be reduced by the action of a general base to remove the proton. Moreover, the resulting alkoxide ion is a much stronger nucleophile than the hydroxyl group.
4. *Protonation of the leaving group*. Similarly, the large negative value of β_{lg} [19] shows that negative charge accumulates on the O5′ leaving group. Protonation of O5′ by a general acid will therefore result in a superior leaving group.

Catalytic strategies 3 and 4 collectively constitute general acid–base catalysis and are generally coordinated. They shall be discussed further in the following section 1.5.

1.5 General Acid–Base Catalysis in Nucleolytic Ribozymes

In specific acid–base catalysis, proton transfer occurs with water (including OH^- and H_3O^+), while general acid–base catalysis involves different (often) organic proton donors and acceptors that are weak acids and bases. In the current context, this means components of the RNA, i.e. nucleobases, 2′-OH groups, or bound hydrated metal ions. It could also involve a bound small molecule acting as a coenzyme, and *glm*S provides one example of this [23–25]. Jenks [26] has drawn attention to the important role of proton transfer in enzymes. In the nucleolytic ribozymes, general acid–base catalysis provides the largest contribution to the catalytic rate enhancement [27]. The most common general base and acid in the nucleolytic ribozymes are nucleobases, and especially that of guanine acting as a general base in the cleavage reaction, but as we shall see, other functionalities can also play a role.

The mechanism of the general acid–base-catalyzed cleavage reaction is shown in Figure 1.3. The general base deprotonates the O2′ nucleophile, and the general acid protonates the 5′-oxyanion leaving group. Some ribozymes catalyze the reverse ligation reaction. In that case by the principle of microscopic reversibility, the general acid and base exchange roles, and their required state of protonation. The catalytic power of macromolecular catalysts employing general acid-base catalysis will be limited by two aspects: the fraction of catalyst that is in an appropriate state of protonation to be active and the reactivity of the general acid and base.

1.5.1 The Fraction of Active Catalyst, and the pH Dependence of Reaction Rates

In the cleavage reaction depicted in Figure 1.3, the general acid must have a proton to donate, and the general base must be able to accept a proton. In other words, to be active, the ribozyme must have a protonated general acid and a deprotonated general base. The observed rate of cleavage (k_{obs}) will be lower than the rate when the ribozyme is fully active (k_{cleave}) according to:

$$k_{obs} = k_{cleave} \cdot f_A \cdot f_B \tag{1.2}$$

where f_A is the fraction of protonated acid and f_B is the fraction of deprotonated base. f_A and f_B will be a function of pH, according to the pK_a values of the general acid and base. pH is arguably the most powerful experimental tool we have in probing general acid–base catalytic mechanisms. For example, the general base can exist either as B^- or BH (e.g. for guanine; the corresponding species for adenine would be B and BH^+) at high and low pH values, respectively. The fraction of the two forms will be given by

$$[B^-]/[BH] = 10^{(pH - pK_a)} \tag{1.3}$$

When the base is operating at a pH that is the same as its pK_a, then half of the molecules will be in the required unprotonated form. If the base has a pK_a = 10, and the reaction is carried out at pH = 7, then most molecules will be protonated (inactive as a base), and only one molecule in 1000 will be in the active unprotonated form. However, we shall see later that this is compensated to some degree by a higher reactivity of the base due to its high pK_a. Similarly, if this moiety is acting as a general acid, then 999 molecules out of 1000 will be in the protonated form that can act as a general acid. But these species will be reluctant to donate that proton, i.e. they will be relatively unreactive.

In the cleavage reactions of the hairpin and Varkud satellite (VS) ribozymes, the general acid and base are the nucleobases of adenine and guanine, respectively (see Chapter 3). The apparent pK_a values (i.e. the values measured from the pH dependence of cleavage rate) in the context of the VS ribozyme reaction have been measured at 5.2 and 8.4, respectively [28]. Neither is close to physiological pH, and we would expect that only one ribozyme molecule in 1000 would be active. Bevilacqua [29] carried out a general analysis for the case of a ribozyme using a general acid and

base (actually formulated for the hairpin ribozyme, but it applies generally), deriving a partition function to calculate f_A and f_B for given values of pK_a:

$$f_A = \left\{1+10^{\left(pK_a^B-pH\right)}\right\} / \left\{1+10^{\left(pK_a^B-pH\right)}+10^{\left(pK_a^B-pK_a^A\right)}+10^{\left(pH-pK_a^A\right)}\right\} \quad (1.4)$$

$$f_B = \left\{1+10^{\left(pH-pK_a^A\right)}\right\} / \left\{1+10^{\left(pK_a^B-pH\right)}+10^{\left(pK_a^B-pK_a^A\right)}+10^{\left(pH-pK_a^A\right)}\right\} \quad (1.5)$$

where the pK_a values of the general acid and base are written pK_a^A and pK_a^B, respectively. Figure 1.4a shows f_A and f_B plotted as a function of pH for the case of pK_a values of 5.2 and 8.4 (simulating the case of the VS ribozyme). At the low pH end, $f_A = 1$ (fully protonated), and then falls in a log-linear manner as the pH rises. Over the same range, f_B rises until it reaches a plateau (fully deprotonated) toward the high pH end. Equation (1.2) shows that the pH dependence of the reaction will reflect the product $f_A \cdot f_B$, that is also plotted in Figure 1.4a. $f_A \cdot f_B$ rises at the low pH end in the regime where $f_A = 1$, but f_B is increasing steadily. It then begins to tail off as f_A begins to fall while f_B is still rising. Eventually, f_B begins to saturate (f_B approaches 1) while f_A is steadily falling in a log-linear fashion. The net result is a bell-shaped curve. It is important to note that the initial rise at low pH is due to deprotonation of the general base, and the fall at high pH is due to general acid deprotonation. However, the reducing rise in $f_A \cdot f_B$ approaching the peak is due to the deprotonation of the acid, not the base.

The shape of this curve fits the experimental data for the VS ribozyme very well (see Chapter 3) [28]. Note that because the general acid has a low pK_a value, the general base has a high pK_a value, and over three units separate the two, the maximum value of $f_A \cdot f_B$ is only 6×10^{-4}. In protein enzymes, the imidazole side chain of histidine is frequently used in general acid–base catalysis. The pK_a of imidazole is normally close to neutrality, so when two histidine residues are used for general acid–base catalysis, a considerably higher value of $f_A \cdot f_B$ is achieved.

The pK_a values for the adenine and guanine nucleobases in the hairpin ribozyme are further apart than those in the VS ribozyme, mostly because the pK_a of guanine in the hairpin ribozyme is higher than that in the VS ribozyme. We have computed an $f_A \cdot f_B$ simulation for pK_a values of 6.0 and 10.0 that corresponds to the hairpin ribozyme in Figure 1.4b. Because the pK_a values are now separated by four units, a distinct plateau forms, where the deprotonation of acid and base compensate in $f_A \cdot f_B$ to create the flat top. Moreover, the eventual fall of $f_A \cdot f_B$ does not occur until a high pH is reached at which measurement of cleavage rate is not possible (i.e. the fall lies in the shaded region of the plot). The overall shape is therefore masked in the experimental profile of rate versus pH, which can therefore be mistaken for a single ionization. This has led to persistent serious errors of interpretation in past studies.

Returning to the case of nucleobases of pK_a values of 5.2 and 8.4, we may ask what pH profile will result for the reverse (ligation) reaction, where the nucleobase of low pK_a acts as a general base in deprotonated form, and that of high pK_a acts are general acid in its protonated form. This is simulated in Figure 1.4c. Now both f_A and $f_B = 1$ over much of the range, and the maximum value of $f_A \cdot f_B = 0.9$. Yet the shape of

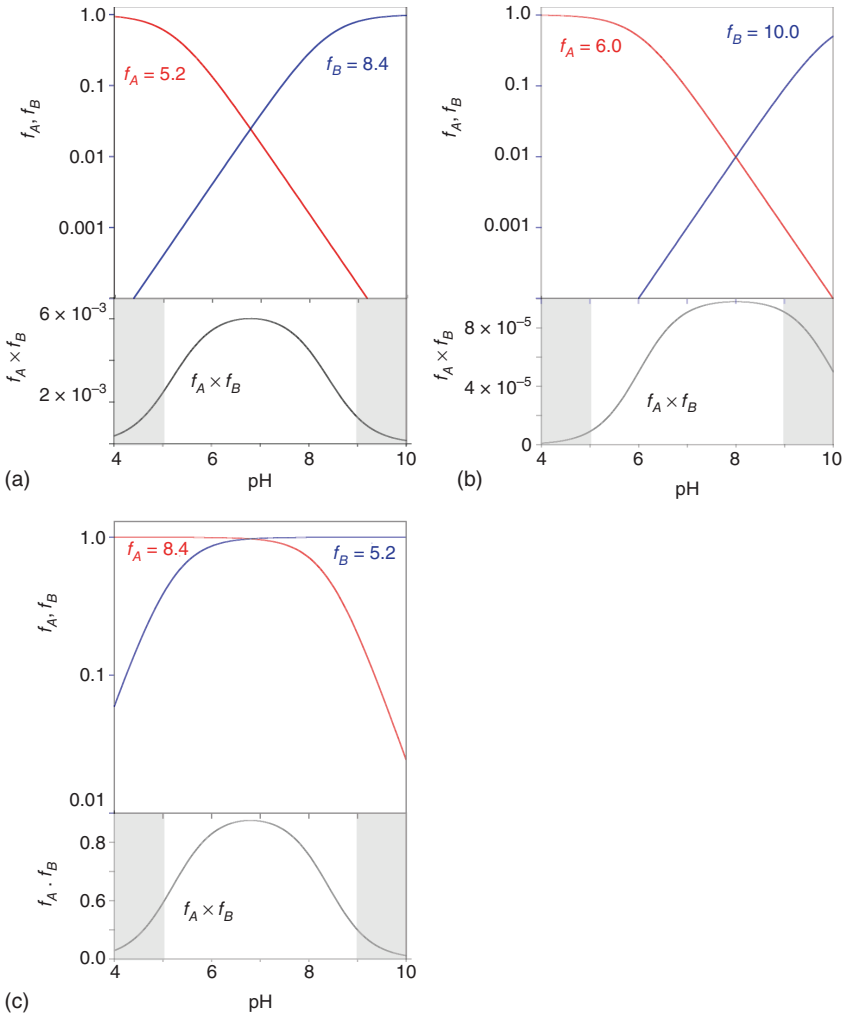

Figure 1.4 Simulations of the pH dependence of general acid–base catalyzed ribozyme reactions. For the three cases shown, the fraction of protonated acid (f_A) and deprotonated base (f_B) have been calculated using Eqs. (1.4, 1.5) and plotted as a function of pH over the range 4–10 (upper plots). The product ($f_A \cdot f_B$) is also plotted as a function of pH (lower plots) with the experimentally inaccessible regions between pH 4–5 and 9–10 shown grayed out. This curve simulates the pH dependence of the reaction rate. These plots have been generated for three cases. (a) $f_A = 5.2$ and $f_B = 8.4$. This generates a bell-shaped curve of $f_A \cdot f_B$ versus pH. This is close to the pH dependence of the VS ribozyme. (b) $f_A = 6.0$ and $f_B = 10.0$. The higher pK_a of the base shifts the reduction in $f_A \cdot f_B$ at higher pH to an inaccessible value, so that the curve appears to reach a stable plateau. This represents the situation with the hairpin ribozyme. (c), $f_A = 8.4$ and $f_B = 5.2$. The pK_a values for the acid and base have been exchanged with respect to part (a). Although the absolute value of $f_A \cdot f_B$ is now higher; the shape of the curve is identical to that in part (a). Thus the pH dependence alone cannot give an assignment of the acid and base; this is known as the principle of kinetic ambiguity.

$f_A \cdot f_B$ versus pH is identical to that where the general base and acid have high and low pK_a values, respectively. This is termed the principle of kinetic ambiguity, and as a consequence, the pH dependence of the reaction cannot reveal which nucleobase is acting as general base and which is the general acid. Other approaches must be used to determine this – see Chapter 3.

Nucleobases participating in proton transfer may also respond to the electrostatic influence of nearby nucleotides that can add complexity to the shape of the pH dependence of reaction rate. Bevilacqua and coworker [30] have recently derived partition functions that take into account cooperative interactions between general acid and base and the effect of titration of nearby nucleotides.

Nucleobase substitution or atomic mutagenesis is generally carried out in conjunction with rate versus pH measurements to investigate the roles for particular functionalities in ribozymes. To take an example, when it was suspected that G630 in the VS ribozyme was acting as the general base in the cleavage reaction, it was substituted by diaminopurine (i.e. replacing O6 by an amine) with a significantly lower pK_a of around 5 [28]. This should shift the curve of f_B versus pH strongly left (i.e. to lower pH) in our simulations, and so the peak of $f_A \cdot f_B$ moves close to pH = 5. The experimental curve followed this closely [28], confirming that the higher pK_a was indeed due to G630. Note, however, that this experiment by itself does not allow us to determine whether G630 is acting as general acid or general base. Similar experiments were performed to probe the role of G33 as a general base in the twister ribozyme [6].

Atomic mutagenesis, coupled with rate versus pH measurements, can provide compelling evidence for the involvement of a given nucleobase. In the twister ribozyme, the adenine (A1) immediately 3′ to the scissile phosphate was suspected to be acting as the general acid in the cleavage reaction, so was subjected to atomic mutagenesis. Replacement of adenine N7 by CH raises its pK_a by about 1.5 units, and it was found that this substitution at A1 raised the rate of cleavage by the twister ribozyme fivefold at pH = 8.5 [22]. While there are a number of ways mutagenesis can lower the catalytic power of a ribozyme, it is much harder to explain how the rate can be increased. But this can be easily rationalized in terms of the fraction of active ribozyme. The A1N7C substitution displaces the curve of f_A versus pH toward that of f_B, raising the peak value of $f_A \cdot f_B$. In this way, the fraction of active catalyst is higher than for the unmodified ribozyme, resulting in a faster-observed rate.

The mechanism of the twister ribozyme illustrates a factor that is normally disregarded. A purine nucleobase has three ring-nitrogen atoms that can be protonated: N3, N7, and N1, in order of decreasing acidity. In other ribozymes, it is N1 that participates in proton transfer, but nucleotide A1 of the twister ribozyme acts as a general acid by donating a proton from the highly acidic N3 [22]. The shape of the rate versus pH curve is determined by the macroscopic pK_a of the nucleobase. However, the relative extent of protonation of the three nitrogen atoms is determined by their respective microscopic pK_as. For adenosine the extent of protonation is N3 0.7%, N7 3.2%, N1 96.1% [31]. Equations (1.2)–(1.5) above assume a single site of protonation, and this is reasonable when N1 participates in proton transfer. However,

to explain the results of atomic mutagenesis for the twister ribozyme, it is necessary to modify Eq. (1.2):

$$k_{\text{obs}} = k_{\text{cleave}} \cdot f_A \cdot f_B \cdot f_{\text{N3H}} \tag{1.6}$$

where f_A and f_B are the fractions of protonated acid and base, respectively, and the extra factor f_{N3H} is the fraction of protonation that occurs specifically at N3 [22].

1.5.2 The Reactivity of General Acids and Bases

We have seen that the nucleobases typically have pK_a values that are removed significantly far from neutrality. Clearly, a disadvantage compared to a protein enzyme using histidine for general acid–base catalysis. Yet the reactivity of these bases is also a function of pK_a, and this works in the opposite sense to the population of the active form, as discussed above. In general base catalysis the rate of ribozyme cleavage is related to the pK_a of the general base by the Brønsted equation:

$$\log\ k_{\text{cleave}} = B - \beta \cdot \text{p}K_a \tag{1.7}$$

where β is the extent of proton transfer in the transition state, and B is a constant specific to the reaction studied. An analogous linear free energy relation can be written for acidity. The activity of an hepatitis delta virus (HDV) ribozyme mutated in the key cytosine nucleotide that acts as the general acid was found to be restored by bases such as imidazole within the solution [32]. A value of $\beta = 0.5$ was calculated by measuring the reaction rate as a function of the pK_a of the exogenous base [33, 34]. Thus the intrinsic rate for a base of p$K_a = 10$ will be 32 times higher than one of p$K_a = 7$. This higher reactivity partially compensates for the small population of unprotonated base that can act in general base catalysis at physiological pH. In the HDV ribozyme experiment, the exogenous base is acting as an acid, so the opposite relationship applies. The intrinsic rate for an acid of p$K_a = 10$ will be 32 times lower than one of p$K_a = 7$, and this is partially offset by the higher population of protonated acid at physiological pH.

1.6 pK_a Shifting of General Acids and Bases in Nucleolytic Ribozymes

The generally accepted pK_a values for the adenine and guanine nucleobases are 4.2 and 9.5, respectively. If they remained at these values in a ribozyme such as the VS then only one molecule in about 10^5 would be in the correct state of protonation to catalyze the cleavage reaction. This fraction could become more favorable if the pK_a values were shifted closer to neutrality, and for the VS ribozyme, apparent values of 5.2 and 8.4 were measured experimentally [28] for the cleavage reaction. Higher values of the lower apparent pK_a have been measured for the hairpin ribozyme as 6.3 [35] and 6.9 for the twister ribozyme [6]. In the context of the electronegative environment of RNA, it is relatively easy to explain raised pK_a values. The most remarkable of these is the twister ribozyme. The adenine (A1) that acts as the general

acid is held in position by a number of hydrogen bonds, two of which involve both protons of N6 that are donated to non-bridging O atoms of successive phosphate groups, that carry a negative charge. It is this unusual environment that raises the pK_a of the adenine virtually three units. This is necessary because, in the catalytic mechanism, it is the highly acidic N3, not the usual N1, that donates a proton to the O5′ oxyanion leaving group (see Chapter 3) [22].

It is harder to see how the pK_a of guanine can be lowered in a ribozyme, and in general, this is less variable. The apparent pK_a of G630 in the VS ribozyme has an unusually low value of 8.4, but this was measured in a high Mg^{2+} concentration. It is quite likely that there is an ion binding site close to G630 [36], and the positively charged ion lowers its apparent pK_a.

1.7 Catalytic Roles of Metal Ions in Ribozymes

Being anionic polyelectrolytes, RNA molecules are associated with many metal ions, some of which may participate directly in catalysis. Both monovalent and divalent metal ions can interact with RNA, although it is the divalent ions that are more likely to bind specifically and function in catalysis. In solution, metal ions are hydrated, with an inner shell of water molecules that are tightly bound. A magnesium ion normally has a first coordination sphere of six water molecules arranged in an octahedral geometry (Figure 1.5). The Mg^{2+}–O distance is 2.1 Å, and according to ligand

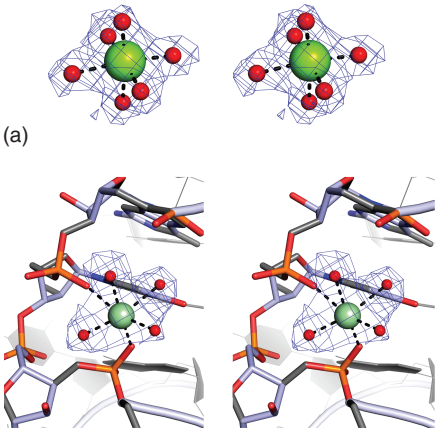

Figure 1.5 Hexaquo-magnesium ions. The Mg^{2+} ion has an inner hydration sphere comprising six tightly bound water molecules with octahedral symmetry. The water molecules may form hydrogen bonds to the RNA or be replaced by RNA ligands such as non-bridging phosphate O atoms. These images are taken from ions bound to ribozyme structures, and the electron density clearly reveals the positions of the hydrating water molecules. These images are shown as parallel-eye stereoscopic pairs. (a) A Mg^{2+} ion with all six inner-sphere water molecules. (b) A Mg^{2+} ion bound to a tight turn in the backbone of the twister ribozyme [6]. This ion has exchanged two inner-sphere water molecules for phosphate non-bridging O atoms, retaining four water molecules of hydration.

field theory, the bond has significant covalent character. These water molecules are not readily displaced, and the great majority of ions associated with RNA retain a full hydration sphere. These are not specifically bound at one location, and exhibit fast exchange. This is termed outer-sphere binding or "atmospheric" binding. Some water molecules within the first hydration sphere may be hydrogen-bonded to acceptors on the RNA, and thus can be located in crystal structures. Monovalent ions virtually always bind as outer-sphere complexes. Most divalent ions such as Mg^{2+} will also be bound in an outer sphere fashion. However, inner-sphere water molecules can sometimes be substituted by one or more RNA ligands (often a non-bridging phosphate O) if a suitable binding pocket can form. In that case, we call this inner-sphere binding, and the complex is in slow exchange. We observed seven hydrated Mg^{2+} ions bound to the twister sister (TS) ribozyme structure [37], all with octahedral symmetry. Two were outer-sphere complexes (retaining full coordination spheres of water molecules), three had exchanged a single inner-sphere water molecule for RNA ligands, and two had exchanged two water molecules. All the RNA ligands were non-bridging phosphate oxygen atoms apart from one where a cytosine O2 was directly bonded to the metal.

Small ions near the top of the periodic table have weakly polarizable orbitals and are classed as "hard" ions. Larger ions with more electrons are more polarizable and are classed as "soft" ions. In general, hard ions bind preferentially to similarly hard anions, so that bound Mg^{2+} ions will normally be found attached to oxygen ligands. By contrast, Mn^{2+} or Cd^{2+} ions bind more avidly to soft atoms like sulfur, and this can be the basis of a way to investigate the roles of metal ions in the transition states of ribozyme reactions.

In general, metal ions are indispensable to the folding of RNA, to lower the electrostatic repulsion between the phosphate groups. In most cases, this can be achieved by monovalent ions, albeit in higher concentration (2 or 3 logs typically) than required for divalent ions, so outer-sphere binding is generally sufficient to achieve folding into the active conformation. However, we sometimes observe that very tight turns in the backbone of RNA may be bridged by an Mg^{2+} ion as an inner-sphere complex (Figure 1.5).

Site-specifically bound metal ions can directly participate in the chemistry of catalysis in a number of different ways:

- They can bind to the reactants and organize and stabilize the structure of the transition state.
- They can stabilize developing negative charge in the transition state electrostatically. An atmosphere of outer-sphere metal ions could also achieve some stabilization of the transition state and, likely, this occurs quite generally in the nucleolytic ribozymes.
- Metal ions can act as Lewis acids, binding directly to reactants to activate them.
- Lastly, hydrated metal ions can act in general acid–base catalysis. Ions like Mg^{2+} are weakly acidic, whereby one of the inner-sphere water molecules can lose a proton, i.e.

$$\left[Mg\left(H_2O\right)_6\right]^{2+} + H_2O \rightleftharpoons \left[Mg\left(H_2O\right)_5OH\right]^{+} + H_3O^{+}$$

with $pK_a = 11.4$. There is good evidence in the HDV ribozyme that a bound metal ion acts as a general base to deprotonate the nucleophilic O2′ [38], the TS ribozyme probably acts in a similar manner [37] (see Chapter 3), and we have recently obtained evidence that a bound metal ion acts as a general acid to protonate the O5′ leaving group of the pistol ribozyme [55].

There are a number of tests that can point to the direct involvement of metal ions in ribozyme chemistry. Ribozymes such as the hairpin or twister are active in high concentrations of monovalent ions, at a rate that is 1/10th of that in Mg^{2+} ions [39]. However, when the metal ion is required to participate directly in the reaction, that factor increases to $\sim 10^{-5}$, e.g. as found in the TS ribozyme [37]. The requirement for inner-sphere coordination can be tested by replacing Mg^{2+} with $Co^{3+}(NH_3)_6$ ions. The two ions are structurally similar, but the ammine ligands of the latter exchange extremely slowly. Thus if inner-sphere ligand exchange is required, $Co^{3+}(NH_3)_6$ cannot replace Mg^{2+} with retention of activity. For example, the HDV ribozyme is essentially inactive in the presence of $Co^{3+}(NH_3)_6$ ions [38].

In contrast to the nucleolytic ribozymes, the larger ribozymes, such as the self-splicing introns and RNaseP, seem to have rejected general acid–base catalysis, in favor of acting as metalloenzymes. Many protein enzymes, including nucleases and polymerases, carry out phosphoryl transfer reactions using two metal ions to activate the nucleophile, position components, and stabilize the transition state [40]. Over a number of years, Herschlag, Piccirilli, and their coworkers explored the role of metal ions in the catalytic mechanism of the group I intron ribozyme using a combination of atomic mutagenesis and careful reaction kinetics [41–46]. Contacts between the metal ions and the transition state were studied by synthesis of sulfur- or amino-substituted substrates (stereo-selectively where relevant), and then looking for restoration of activity using softer metal ions such as Mn^{2+} or Cd^{2+}. This is often termed metal ion rescue. These experiments indicated that three metal ions are bound to the transition state of the group I intron ribozyme (Figure 1.6a). These are:

- *Metal ion A*. Bound to the 3′ and *pro*S non-bridging O atoms of the scissile phosphate. This probably functions by stabilizing the transition state as a negative charge develops on the leaving group.
- *Metal ion B*. Bound to the O3′ of the guanosine. This interaction would be expected to activate the nucleophile, possibly acting as a Lewis acid.
- *Metal ion C*. Bound to the O2′ of the guanosine plus the *pro*S non-bridging O of the scissile phosphate. Here the role is less obvious, but the metal ion could serve to position the reacting groups, as well as providing further electrostatic stabilization.

Two metal ions were observed bound in the active site of the *Azoarcus* group I intron ribozyme poised at the second stage [47, 48] (Figure 1.6b). One was bound to the 3′ and *pro*S non-bridging O atoms of the scissile phosphate, i.e. as deduced for metal ion A. The other was bound like a combination of metal ions B and C, interacting with O2′ and O3′ of the guanosine as well as the *pro*S non-bridging O of the scissile. The difference between the conclusions from structural and functional studies could reflect disorder within the crystal, or perhaps a difference between

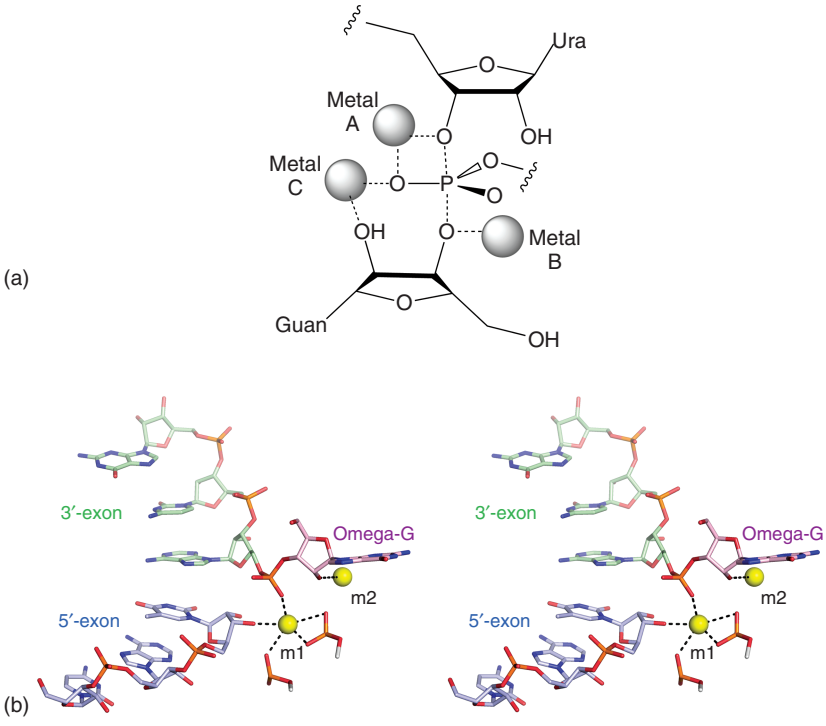

Figure 1.6 The positions of Mg^{2+} ions bound in the transition state of the group I intron ribozyme. (a) The locations of divalent metal ions deduced from systematic analysis of the kinetics of ribozymes with atomic substitutions (especially S for O) coupled with the exchange of Mg^{2+} for softer metal ions [41–46]. (b) Parallel-eye stereoscopic view of the crystal structure of the *Azoarcus* group I intron ribozyme trapped prior to the second step of the splicing reaction [47]. The 3′-OH of the 5′-exon is poised to make a nucleophilic attack on the adjacent phosphodiester linkage in the 3′-exon, leaving the terminal guanine nucleotide (Ω-G) bound to the ribozyme. Two metal ions (m1 and m2) are coordinated in the active center. m1 is directly bound to the O3′ nucleophile.

a necessarily ground-state structure and kinetic measurements that can probe the transition state.

1.8 The Choice Between General Acid–Base Catalysis and the Use of Metal Ions

The majority of ribozymes use either general acid–base catalysis or act as metalloenzymes. The same division of catalytic mechanism is found in protein enzymes performing phosphoryl transfer reaction. RNaseA uses histidine side chains to remove and donate protons [49, 50] while a typical restriction enzyme uses Mg^{2+} ions. All nucleolytic ribozymes seem to use general acid–base catalysis, where nucleobases frequently adopt the role taken by histidine in RNaseA (Chapter 3). By contrast, RNaseP and the self-splicing introns have generally evolved metal

ion-based catalytic mechanisms. The reason for the distinction is not clear. An active center in which metal ions play the key catalytic role may be more amenable to remodeling in between two-stage reactions like those of the group I and II introns. It is perhaps easier to evolve an RNA that uses bound metal ions, given its polyanionic nature. No ribozyme derived by in vitro selection has proved to use nucleobases, and the close similarity of the active sites of the hairpin and VS ribozymes (Chapter 3) suggests there could be relatively few ways to use nucleobases to catalyze phosphoryl transfer reactions.

1.9 The Limitations to RNA Catalysis

By comparison with proteins, the catalytic resources of RNA are very limited. These are just four rather similar heterocyclic nucleobases, 2′-hydroxyl groups, and hydrated metal ions. This is perhaps reflected in the catalytic rate enhancements achieved and the limited range of reactions that are catalyzed. Part of the limitation comes from the pK_a values of the nucleobases; for example, only a small fraction of the VS ribozyme carrying out cleavage is active at a given time. If due allowance is made for that, then the catalytic efficiency becomes comparable to RNaseA [51]. Rate could well be a limitation, and the majority of ribozymes that exist in contemporary cells do not undergo multiple turnovers.

The lack of a wide array of chemical resources may be a greater limitation on the range of chemistry catalyzed. In the RNA world hypothesis, it is necessary that RNA would catalyze a much greater range of chemistry. We can speculate that the chemical repertoire of RNA might be expanded if small molecules could bind and act as coenzymes. RNA is very good at binding small molecule ligands with great specificity, exemplified by the great range of ligands for the riboswitches [52]. Riboswitches have been identified that bind a number of coenzymes, including thiamine pyrophosphate (TPP), flavin mononucleotide (FMN), *S*-adenosylmethionine (SAM), S-adenosylhomocysteine (SAH), tetrahydrofolate (THF), Ado-cobalamine. GlmS (Chapter 3) provides a precedent for a ribozyme using a coenzyme, where bound glucosamine-6-phosphate is the probable general acid in the cleavage reaction. The most abundant group of riboswitches are those that bind TPP [53]. TPP is a very versatile coenzyme, involved in the formation and breakage of carbon–carbon bonds, e.g. in transketolase. As we have discussed previously [54], we should consider the possibility that a ribozyme might bind TPP as a coenzyme, to catalyze a new range of metabolic interconversions. The discovery of such novel ribozymes would be exciting indeed!

Acknowledgment

Work on RNA catalysis in Dundee is funded by Cancer Research UK under program Grant A18604.

References

1 Seelig, B. and Jäschke, A. (1999). A small catalytic RNA motif with Diels–Alderase activity. *Chem. Biol.* 6 (3): 167–176.
2 Sengle, G., Eisenfuh, R.A., Arora, P.S. et al. (2001). Novel RNA catalysts for the Michael reaction. *Chem. Biol.* 8 (5): 459–473.
3 Tsukiji, S., Pattnaik, S.B., and Suga, H. (2003). An alcohol dehydrogenase ribozyme. *Nat. Struct. Biol.* 10 (9): 713–717.
4 Khvorova, A., Lescoute, A., Westhof, E., and Jayasena, S.D. (2003). Sequence elements outside the hammerhead ribozyme catalytic core enable intracellular activity. *Nat. Struct. Biol.* 10 (9): 1–5.
5 Martick, M. and Scott, W.G. (2006). Tertiary contacts distant from the active site prime a ribozyme for catalysis. *Cell* 126 (2): 309–320.
6 Liu, Y., Wilson, T.J., McPhee, S.A., and Lilley, D.M. (2014). Crystal structure and mechanistic investigation of the twister ribozyme. *Nat. Chem. Biol.* 10 (9): 739–744.
7 Rupert, P.B., Massey, A.P., Sigurdsson, S.T., and Ferré-D, Amaré, A.R. (2002). Transition state stabilization by a catalytic RNA. *Science* 298 (5597): 1421–1424.
8 Mir, A. and Golden, B.L. (2016). Two active site divalent Ions in the crystal structure of the hammerhead ribozyme bound to a transition state analogue. *Biochemistry* 55 (4): 633–636.
9 Evans, M.G. and Polyani, M. (1935). Some applications of the transition state method to the calculation of reaction velocities, especially in solution. *Trans. Faraday Soc.* 31: 875–894.
10 Eyring, H. (1935). The activated complex in chemical reactions. *J. Chem. Phys.* 3: 107–114.
11 Pelzer, H. and Wigner, E. (1935). Über die geschwindigkeitskon stante von austauschreaktionen *Z. Phys. Chem.* B15: 445.
12 Oivanen, M., Kuusela, S., and Lonnberg, H. (1998). Kinetics and mechanisms for the cleavage and isomerization of the phosphodiester bonds of RNA by Brönsted acids and bases. *Chem. Rev.* 98 (3): 961–990.
13 Rupert, P.B. and Ferré-D'Amaré, A.R. (2001). Crystal structure of a hairpin ribozyme-inhibitor complex with implications for catalysis. *Nature* 410: 780–786.
14 Westheimer, F.H. (1968). Pseudo-rotation in the hydrolysis of phosphate esters. *Acc. Chem. Res.* 1: 70–78.
15 van Tol, H., Buzayan, J.M., Feldstein, P.A. et al. (1990). Two autolytic processing reactions of a satellite RNA proceed with inversion of configuration. *Nucleic Acids Res.* 18 (8): 1971–1975.
16 Slim, G. and Gait, M.J. (1991). Configurationally defined phosphorothioate-containing oligoribonucleotides in the study of the mechanism of cleavage of hammerhead ribozymes. *Nucleic Acids Res.* 19 (6): 1183–1188.
17 Gerratana, B., Sowa, G.A., and Cleland, C.W. (2000). Characterization of the transition-state structures and mechanisms for the isomerization and cleavage reactions uridine 3′-m-nitrobenzyl phosphate. *J. Am. Chem. Soc.* 122 (51): 12615–12621.

18 Ye, J.D., Li, N.S., Dai, Q., and Piccirilli, J.A. (2007). The mechanism of RNA strand scission: an experimental measure of the Brønsted coefficient, beta nuc. *Angew. Chem.* 46 (20): 3714–3717.

19 Kosonen, M., Youseti-Salakdeh, E., Strömberg, R., and Lönnberg, H. (1997). Mutual isomerization of uridine 2′- and 3′-alkylphosphatesand cleavage to a 2′,3′-cyclic phosphate: the effect of the alkyl group on the hydronium and hydroxide-ion-catalyzed reactions. *J. Chem. Soc. Perkin Trans.* 2: 2661–2666.

20 Soukup, G.A. and Breaker, R.R. (1999). Relationship between internucleotide linkage geometry and the stability of RNA. *RNA* 5 (10): 1308–1325.

21 Koo, S., Novak, T., and Piccirilli, J.A. (2008). Catalytic mechanism of the HDV ribozyme. In: *Ribozymes and RNA Catalysis* (eds. D.M.J. Lilley and F. Eckstein). Cambridge: Royal Society of Chemistry.

22 Wilson, T.J., Liu, Y., Domnick, C. Kath-Schorr, S. and D. M. J. Lilley, D. M. J. (2016). The novel chemical mechanism of the twister ribozyme. *J. Am. Chem. Soc.* 138 (19): 6151–6162.

23 McCarthy, T.J. Plog, M. A., Floy, S. A., Jansen, J. A., Soukup, J. K. and Soukup, G. A. (2005). Ligand requirements for glmS ribozyme self-cleavage. *Chem. Biol.* 12 (11): 1221–1226.

24 Klein, D.J. and Ferré-D'Amaré, A.R. (2006). Structural basis of glmS ribozyme activation by glucosamine-6-phosphate. *Science* 313 (5794): 1752–1756.

25 Cochrane, J.C., Lipchock, S.V., Smith, K.D., and Strobel, S.A. (2009). Structural and chemical basis for glucosamine 6-phosphate binding and activation of the glmS ribozyme. *Biochemistry* 48 (15): 3239–3246.

26 Jenks, W.P. (1987). *Catalysis in Chemistry and Enzymology*. New York: Dover Publications Inc.

27 Li, Y. and Breaker, R.R. (1999). Kinetics of RNA degradation by specific base catalysis of transesterification involving the 2′-hydroxyl group. *J. Am. Chem. Soc.* 121: 5364–5372.

28 Wilson, T.J., McLeod, A.C., and Lilley, D.M.J. (2007). A guanine nucleobase important for catalysis by the VS ribozyme. *EMBO J.* 26 (10): 2489–2500.

29 Bevilacqua, P.C. (2003). Mechanistic considerations for general acid–base catalysis by RNA: revisiting the mechanism of the hairpin ribozyme. *Biochemistry* 42 (8): 2259–2265.

30 Frankel, E.A. and Bevilacqua, P.C. (2018). Complexity in pH-dependent ribozyme kinetics: dark pK_a shifts and wavy rate-pH profiles. *Biochemistry* 57 (5): 483–488.

31 Kapinos, L.E., Operschall, B.P., Larsen, E., and Sigel, H. (2011). Understanding the acid–base properties of adenosine: the intrinsic basicities of N1, N3 and N7. *Chemistry* 17 (29): 8156–8164.

32 Perrotta, A.T., Shih, I., and Been, M.D. (1999). Imidazole rescue of a cytosine mutation in a self-cleaving ribozyme. *Science* 286 (5437): 123–126.

33 Shih, I.H. and Been, M.D. (2001). Involvement of a cytosine side chain in proton transfer in the rate-determining step of ribozyme self-cleavage. *Proc. Natl. Acad. Sci. U.S.A.* 98 (4): 1489–1494.

34 Nakano, S., Proctor, D.J., and Bevilacqua, P.C. (2001). Mechanistic characterization of the HDV genomic ribozyme: assessing the catalytic and structural contributions of divalent metal ions within a multichannel reaction mechanism. *Biochemistry* 40 (40): 12022–12038.

35 Nahas, M.K. et al. (2004). Observation of internal cleavage and ligation reactions of a ribozyme. *Nat. Struct. Mol. Biol.* 11 (11): 1107–1113.

36 Zamel, R. and Collins, R.A. (2002). Rearrangement of substrate secondary structure facilitates binding to the *Neurospora* VS ribozyme. *J. Mol. Biol.* 324 (5): 903–915.

37 Liu, Y., Wilson, T.J., and Lilley, D.M.J. (2017). The structure of a nucleolytic ribozyme that employs a catalytic metal ion. *Nat. Chem. Biol.* 13: 508–513.

38 Nakano, S., Chadalavada, D.M., and Bevilacqua, P.C. (2000). General acid–base catalysis in the mechanism of a hepatitis delta virus ribozyme. *Science* 287: 1493–1497.

39 Murray, J.B., Seyhan, A.A., Walter, N.G. et al. (1998). The hammerhead, hairpin and VS ribozymes are catalytically proficient in monovalent cations alone. *Chem. Biol.* 5: 587–595.

40 Steitz, T.A. and Steitz, J.A. (1993). A general 2-metal-ion mechanism for catalytic RNA. *Proc. Natl. Acad. Sci. U.S.A.* 90 (14): 6498–6502.

41 Shan, S.O., Yoshida, A., Sun, S.G. et al. (1999). Three metal ions at the active site of the *Tetrahymena* group I ribozyme. *Proc. Natl. Acad. Sci. U.S.A.* 96 (22): 12299–12304.

42 Shan, S., Kravchuk, A.V., Piccirilli, J.A., and Herschlag, D. (2001). Defining the catalytic metal ion interactions in the *Tetrahymena* ribozyme reaction. *Biochemistry* 40 (17): 5161–5171.

43 Forconi, M., Lee, J., Lee, J.K. et al. (2008). Functional identification of ligands for a catalytic metal ion in group I introns. *Biochemistry* 47 (26): 6883–6894.

44 Forconi, M., Sengupta, R.N., Piccirilli, J.A., and Herschlag, D. (2010). A rearrangement of the guanosine-binding site establishes an extended network of functional interactions in the Tetrahymena group I ribozyme active site. *Biochemistry* 49 (12): 2753–2762.

45 Sengupta, R.N., Herschlag, D., and Piccirilli, J.A. (2012). Thermodynamic evidence for negative charge stabilization by a catalytic metal ion within an RNA active site. *ACS Chem. Biol.* 7 (2): 294–299.

46 Sengupta, R.N. et al. (2016). An active site rearrangement within the *Tetrahymena* group I ribozyme releases nonproductive interactions and allows formation of catalytic interactions. *RNA* 22 (1): 32–48.

47 Adams, P.L., Stahley, M.R., Wang, J., and Strobel, S.A. (2004). Crystal structure of a self-splicing group I intron with both exons. *Nature* 430: 45–50.

48 Stahley, M.R. and Strobel, S.A. (2005). Structural evidence for a two-metal-ion mechanism of group I intron splicing. *Science* 309 (5740): 1587–1590.

49 Thompson, J.E. and Raines, R.T. (1994). Value of general acid–base catalysis to ribonuclease A. *J. Am. Chem. Soc.* 116: 5467–5468.
50 Raines, R.T. (1998). Ribonuclease A. *Chem. Rev.* 98 (3): 1045–1066.
51 Wilson, T.J. et al. (2010). Nucleobase-mediated general acid–base catalysis in the Varkud satellite ribozyme. *Proc. Natl. Acad. Sci. U.S.A.* 107: 11751–11756.
52 Breaker, R.R. (2011). Prospects for riboswitch discovery and analysis. *Mol. Cell* 43 (6): 867–879.
53 Winkler, W., Nahvi, A., and Breaker, R.R. (2002). Thiamine derivatives bind messenger RNAs directly to regulate bacterial gene expression. *Nature* 419 (6910): 952–956.
54 Wilson, T.J. and Lilley, D.M.J. (2015). RNA catalysis – is that it? *RNA* 21 (4): 534–537.
55 T. J. Wilson, Y. Liu N. S. Li, Q. Dai, J. A. Piccirilli and D. M. J. Lilley (2019). Comparison of the structures and mechanisms of the pistol and hammerhead ribozymes. *J. Amer. Chem. Soc* 141, 7865–7875.